UNCLASSIFIED

APAE-3(Del.)

Work performed under Contract No. AT(11-1)-318

SHIELDING REQUIREMENTS

FOR THE

ARMY PACKAGE POWER REACTOR

May 1, 1956

J. L. Meem

F B. Fairbanks

Alco Products, Inc.
Schenectady, New York

Photostat Price $10.80

Microfilm Price $3.90

Available from the
Office of Technical Services
Department of Commerce
Washington 25, D. C.

UNCLASSIFIED

DISCLAIMER

ACKNOWLEDGEMENTS

Important contributions to the shield design were made by A. H. Fox, to the general arrangement by K. Kasschau, and to the calculations by F. Abernathy. The work of the staff of the Atomic Energy Engineering Department in the preparation of the report is gratefully acknowledged.

ABSTRACT

The design, selection, and calculation of the Army Package Power Reactor shielding are described.

The APPR-1, a prototype of a package reactor for remote locations, has a primary shield of iron and water. This shield has been adopted to permit fast erection and to provide low transported weight. Economically, including transportation cost, the iron water shield is better than a lead water shield and is competitive with a concrete shield for a remote site.

Because of its location at Fort Belvoir, Va., the shielding requirements for the APPR-1 are considerably more stringent than those for a reactor at a remote base. Since the secondary shielding which surrounds the entire primary system must provide protection for personnel at any location outside the vapor container, concrete is provided for this need.

APAE-3

SHIELDING REQUIREMENTS FOR THE ARMY PACKAGE POWER REACTOR

TABLE OF CONTENTS

CHAPTER 1

GENERAL DESIGN CONSIDERATIONS

1.1 Introduction

The Army Package Power Reactor will be designed, constructed and operated for the first six months by ALCO Products, Inc. on contract with the Army Reactors Branch of the A.E.C. The APPR-1 is a prototype of a reactor designed to meet the requirements and site conditions of a remote military base. Since the prototype reactor is to be constructed at a site in the United States, some of the design requirements were changed to meet these needs. In particular, containment of the maximum credible accident is provided.

The APPR-1 is a 10,000-kilowatt pressurized water reactor delivering 1825 kilowatts of electricity, with 85° F. condenser cooling water. The fuel elements are similar to those in the MTR but are made of stainless steel rather than aluminum and in addition to the fissionable material contain a burnout poison in the form of boron

The reactor operates at a pressure of 1200 psi and outlet temperature of 450° F at full power The water flows from the reactor to a steam generator where heat is transferred to the secondary steam system. From the steam generator the primary water flows through the pump to the reactor inlet. The entire primary loop is installed inside a vapor container, 32 feet in diameter and 60 feet high, as shown in the cutaway drawing, Fig. 1 1, and

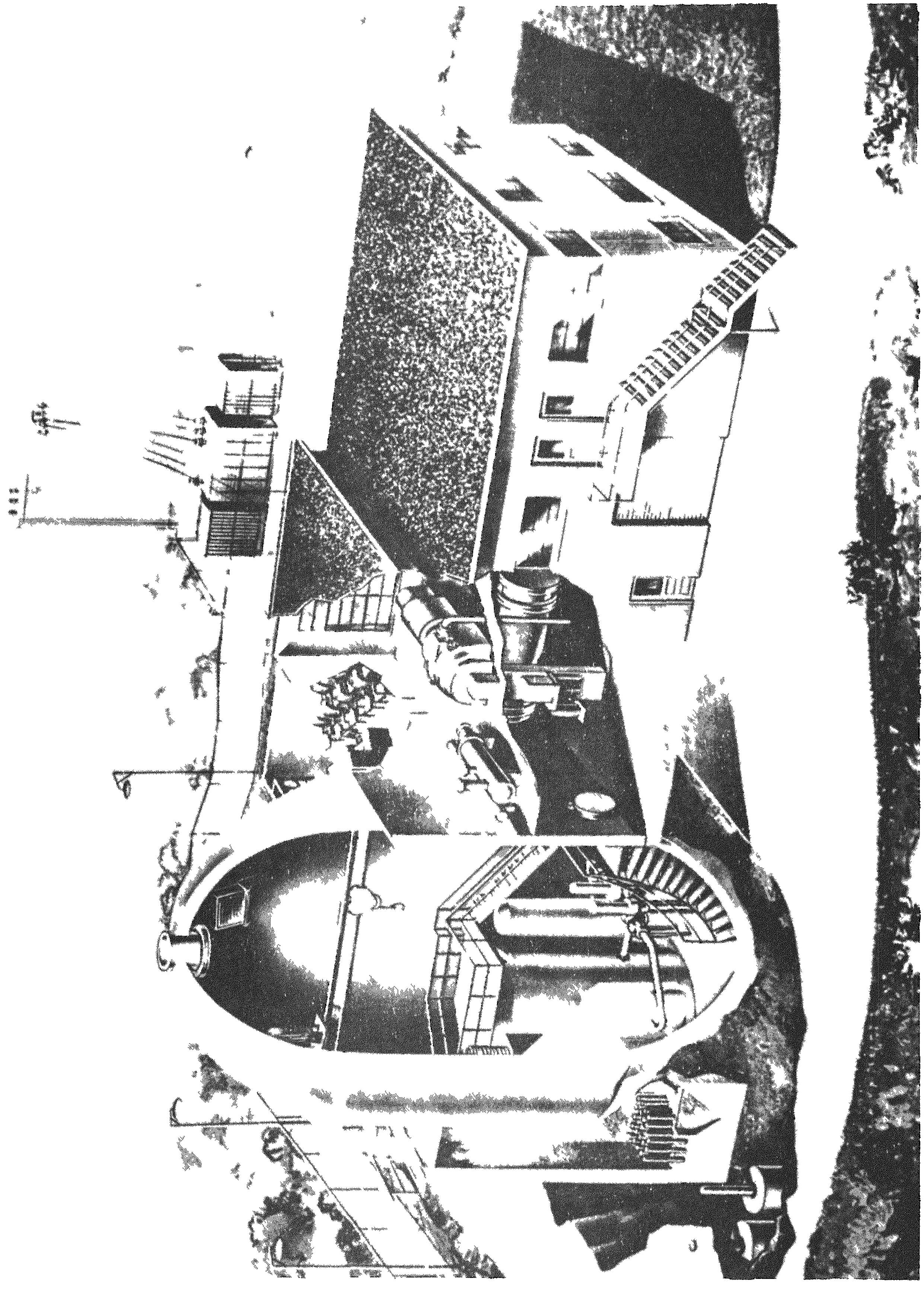

FIG. 1.1 - CUTAWAY DRAWING OF APPR-1 PLANT

in the elevation and plan views, Figs. 1.2 and 1.3. The vapor container consists of a 7/8" steel cylindrical outer shell with hemispherical ends, designed to contain the energy released from all of the steam generated by flashing of the superheated primary and secondary system water volumes when the maximum amount of heat has been stored in these volumes. Inside this shell a 2 foot thickness of reinforced concrete is included for missile protection and shielding. The concrete provides a rupture proof container which will contain missiles that might result from failure of the high pressure primary system. An additional 3 feet of concrete for shielding surrounds the vapor container as high as the ceiling of the control room.

1.2 Objectives of the Shield Design

In designing the APPR-1 shielding, the objective has been to provide sufficient shielding to meet the accepted practices throughout the Atomic Energy Commission program for radiation levels for operating personnel. Under normal operating conditions, levels for personnel continuously exposed during working hours are restricted to a fraction of the accepted permissible level of 300 mr per week. In certain areas, however, above-tolerance levels are permitted where infrequent access is required for periods of controlled short duration. Taking advantage of this fact permits somewhat greater flexibility of design and operation but at no expense in terms of increased hazard to the operating personnel.

While it is desired to achieve as much of a prototype in the shield design as it is possible to do, one basic compromise was introduced by the

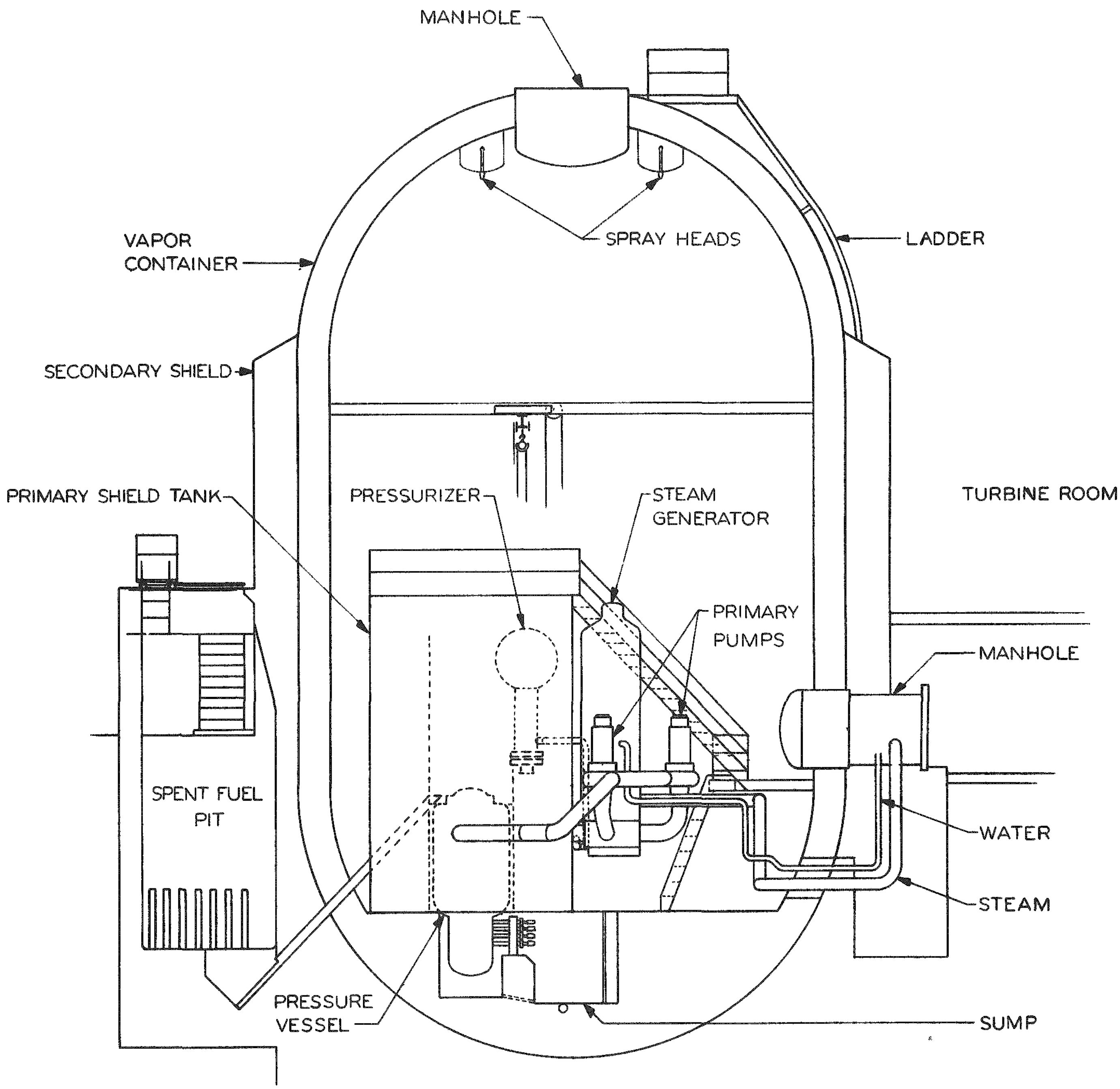

FIG. 1.2 - VAPOR CONTAINER ELEVATION

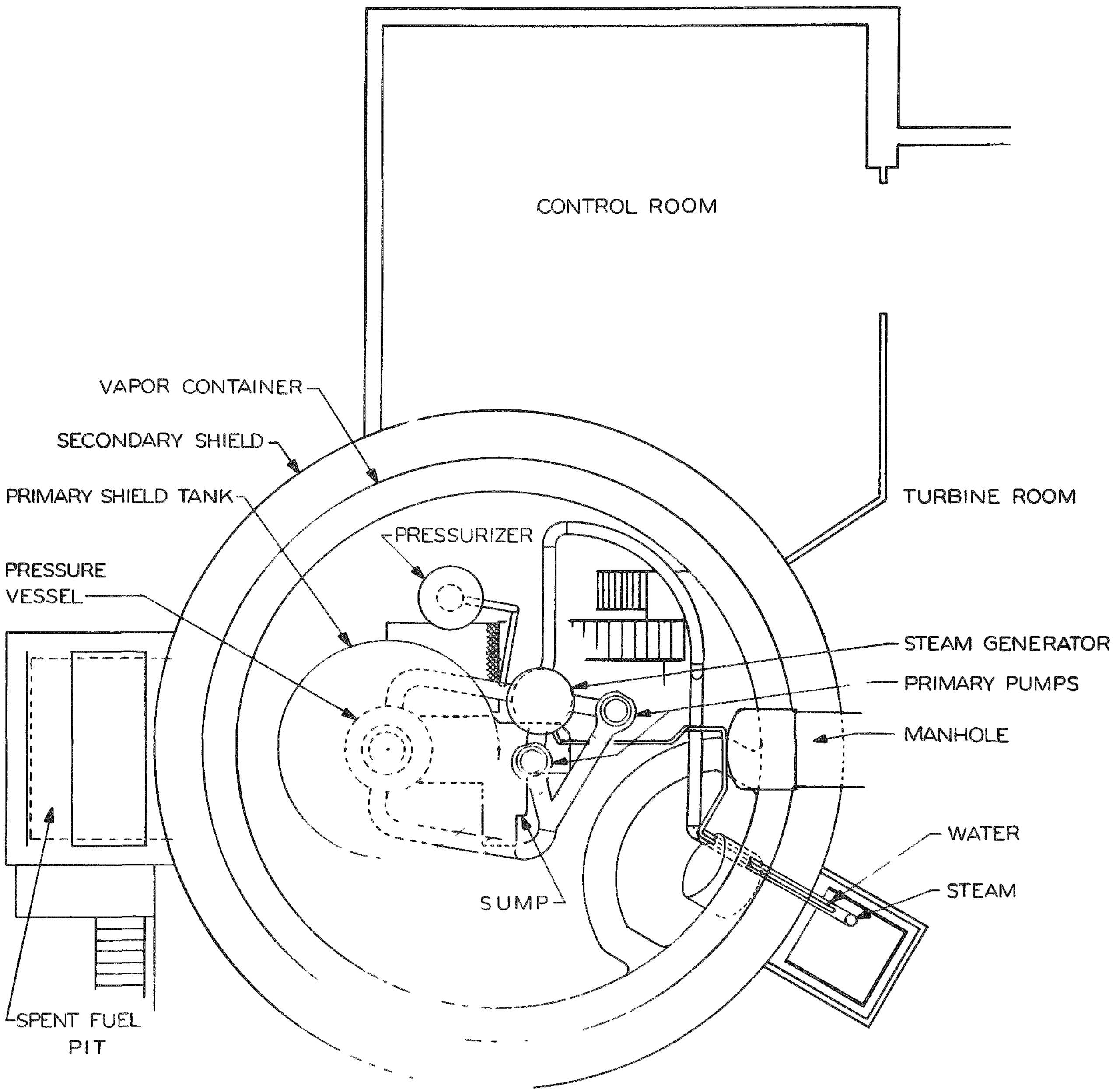

FIG. 1.3 - VAPOR CONTAINER PLAN VIEW

desire to locate the facility at Fort Belvoir. In a location such as Fort Belvoir, it is necessary to provide a facility which can be approached at any time and from any angle without being unwittingly exposed to excessive radiation levels. Thus the radiation existing at any point around the building will be no higher than the permissible continuous exposure level. This will not only make it possible for modifications to the facility to be considered at a later date with impunity, but it will also render unnecessary a close policing of visitors to prevent them from wandering into areas where the radiation dose level may be above tolerance.

In contrast with the above, the design of an actual facility for use in remote areas could easily take advantage of the distance factor as a means for providing shielding on those sectors of the reactor compartment where no access is required during operation. In such an installation it would be proposed to provide minimal shielding in these sectors and prevent access to dangerous areas by means of fences or natural obstructions. Such a technique will provide for minimum transportable shield weight, yet the danger to personnel will be trivial due to the close control over the personnel in the vicinity of such an actual installation.

As indicated above, the basic shield design for the APPR-1 is to provide adequate protection for plant personnel under any and all operating conditions normal to a plant of this type. A primary shield is provided around the reactor pressure vessel which reduces the gamma rays from the core to a level comparable to the intensity of those gammas arising in the activated water external to the shield. This primary shield also provides the necessary attenuation for capture gamma rays and reduces the neutron level to a point where no significant activation of the equipment outside the shield occurs.

Besides the two feet of concrete in the walls of the vapor container, there are three additional feet of concrete as high as the ceiling of the control room. The secondary shield provided by this five feet of concrete brings the dose rate down to two-tenths tolerance in the control room.

The principal source of gamma rays in the primary water is from the O^{16} (n, p) N^{16} reaction. Since the half life of N^{16} is only seven seconds, access may be had to the vapor container within a reasonable period of time after shutdown. The shutdown activity in the primary coolant water will result from the impurities present in the system, which result from pick-up of corrosion products and impurities in the makeup water.

CHAPTER 2

SECONDARY SHIELD

2.1 Design

The secondary shield is described in Table 2.1. It is designed so that radiation from the primary coolant would give not more than one-tenth of laboratory tolerance for a 40-hour week at any point outside the vapor container up to the full height of the power plant building. The dose rate at a position outside the vapor container due to important primary coolant components is indicated in Table 2.2. Small volumes of primary coolant, such as in the pump, are conservatively assumed in the 12-feet of primary piping.

Penetrations of the secondary shield by the steam line and several smaller lines are shielded by placing sufficient material around the openings to compensate for the concrete removed. The steam line is oriented so as not to be in a direct line with any major radiation source.

2.2 Sources of Primary Coolant Activity

The only significant coolant activity during reactor operation is that of N^{16}. The neutron source from the decay of N^{17} produced by the 0^{17} (n,p) N^{17} reaction is lower by several orders of magnitude than the gamma source from N^{16}. These neutrons are readily attenuated to a negligible dose by 5 feet of concrete.

The equation used to calculate the activation of 0^{16} circulating through a neutron flux for a long time is:

TABLE 2.1

SECONDARY SHIELDING

Description	Material	Outer Radius Inches	Thickness Inches
Vapor Container Lining	Steel	204.1	0.1
Vapor Container Structure	Concrete	224.1	24.0
Vapor Container Wall	Steel	225.0	0.9
Secondary Shield *	Concrete	261.0	36.0

* To a height of 27 ft. above ground level.

TABLE 2.2

DOSE RATE OUTSIDE VAPOR CONTAINER FROM PRIMARY COOLANT ACTIVITY DURING REACTOR OPERATION

Source	Diameter Inches	Length Inches	Distance from Center to Outside of Shield Near Control Room Feet
Piping	11	144	18
Steam Generator Bundle	44	144	22
Steam Generator Channel	33	18	22

Source	Gamma Flux Outside Shield Photons/cm^2-sec.	Gamma Dose Rate Outside Shield Mr/hr
Piping	40	0.31
Steam Generator Bundle	43	0.33
Steam Generator Channel	16	0.12
Total	99	0.76

$$A(O) = \Sigma_a \phi \frac{1-e^{-\lambda t_r}}{1-e^{-\lambda t_c}}$$

where: $A(O)$ = activity at the core outlet, dis/sec/cc

Σ_a = activation cross section, cm^{-1}

ϕ = activation flux, n/cm^2 sec

λ = disintegration constant, $sec^{-1} = 0.0943$

t_c = time for one complete cycle, sec = 17.5

t_r = time in active zone, sec = 0.582 (based on a 30" active zone)

One estimate of 0^{16} (n, p) N^{16} cross section is 38 microbarns (1) which is to be used with the fission neutron flux. The cross section as a function of energy has been measured by Martin (2). An average of this cross section over Watts fission spectrum gives 26 microbarns (3). For conservatism, the 38 microbarn cross section is used.

In the reactor the 0^{16} is activated both in the core and reflector. Measurements have been made on the Bulk Shielding Reactor (BSR) with the fast neutron dosimeter at various distances from the core [4]. This fast flux is used to estimate the average fission neutron flux in the core and reflector. The fission neutron flux in the core is estimated to be twice the fast neutron flux measured at the edge of the BSR. The average flux in the reflector is found by fitting the BSR data with an exponential and integrating over the APPR reflector.

$$\phi\,(\text{core}) = 5 \times 10^6\ n/cm^2/sec/watt$$

$$\phi\,(\text{reflector}) = 0.63 \times 10^6\ n/cm^2/sec/watt$$

About one-half of the coolant flows thru the reflector and the residence time in the reflector is estimated to be [illegible] sec. The activity at the core outlet due to the flow thru the reflector is [illegible] in the core and reduced by one half because of mixing.

The activity at the core outlet [illegible]

A (O) = [illegible] core

A (O) = [illegible] reflector

A (O) = [illegible] total

The previous estimate of [illegible] (6) was 1.63 x 10^6 dis/sec/cm^3 which was based on [illegible] the [illegible] activity for the difference in [redacted] power [illegible]

It is [illegible] consider [illegible] equation presented by Binford[3] based on experimental measurements on the LITR.

$$C\ (\text{dis/sec/cc}) = \frac{1.04 \times 10^9}{K}$$

where:

K = flow rate GPM/MW

In the table below is the result of applying this equation to the APPR-1, LITR and STR together with experimental measurements on the LITR and STR.

Reactor	K	Binford Eq	Activity, Dis/sec/cm^3 Calculation	Experiment
APPR	[illegible]	2 [illegible] x 10^6	4 [illegible] x 10^6	
LITR	[illegible]	2. [illegible] x 10^6	1.6 x [illegible]	2.6 x 10^6 (3)
STR	[illegible]	4.5 [illegible] x 10^6	4.4 x 10^6 (8)	6.6 x 10^6

2.3 Shielding of Primary Coolant Activity During Reactor Operation

Three volume sources are considered: steam generator tube bundle, steam generator channel and piping.

CONFIDENTIAL

DECLASSIFIED

The steam generator tube bundle is idealized as a right circular cylinder 44" in diameter and 12 ft. high. The contents are assumed to be 740 steel tubes of the correct size, filled with primary coolant. The shell side of the steam generator is considered empty. The material is made homogeneous throughout the cylinder. This condition is chosen to represent the source from the superheater segment. This space is approximately 12 ft. high and is essentially void on the shell side. The homogenized source has an effective iron density of 0.536 and water density of 0.122 gm/cc.

The steam generator channel is taken as a right circular cylinder 18 [illegible] and 33" in diameter, filled with primary coolant.

The piping is assumed to be a right circular cylinder 11" in diameter, 12 ft long. This length includes bends external to the primary shield tank and small volumes in pumps and check valve.

The above dimensions are summarized in Table 2.2

Shielding

The shielding around each source is tabulated below:

Source	Steam Generator Tube Bundle	Steam Generator Channel	Piping
	(inches of iron)		
Wall Thickness	0 75	0.312	[illegible]
	(inches of concrete)		
Vapor Container	60	80	[illegible]

The gamma mass absorption coefficients are obtained from Reference 4 for water and iron and from extrapolation of data from Reference 23 for concrete. The following absorption coefficients are used.

Material	Density gm/cm^3	Mass Absorption Coefficient for 6.7 Mev Gammas, cm^{-1}
Primary Coolant	0.83	0.0214
Vessel Walls	7.85	0.237
Concrete	2.3	0.0599
Steam Generator Tube Bundle (homogeneous)	0.658	0.0194

Method of Calculation

The gamma flux can be obtained from the formula.

$$\phi_\gamma = B \frac{Q_v \quad C^2}{2(a + Z)} F(\phi, b)$$

where:

B = dose buildup factor

ϕ_γ = gamma flux - photons/cm^2/sec.

Q_v = volume source strength - photons/cc/sec.

C = radius of cylindrical source - cm

Z = effective self absorption distance - cm

b = $\sum \mu_i t_i + \mu_s Z$

μ_i = absorption coefficient of ith material - cm^{-1}

μ_s = absorption coefficient of source - cm^{-1}

t_i = thickness of ith material - cm

a, ϕ = are dimensions as indicated in Fig 2 1

$$F(\phi, b) = \int_0^{\phi} e^{-b \sec \phi} \, d\phi$$

The functions Z and $F(\phi, b)$ are shown in Reference (9)

It should be noted that the volume source strength for the steam generator tube bundle is obtained by correcting the volume source strength as calculated

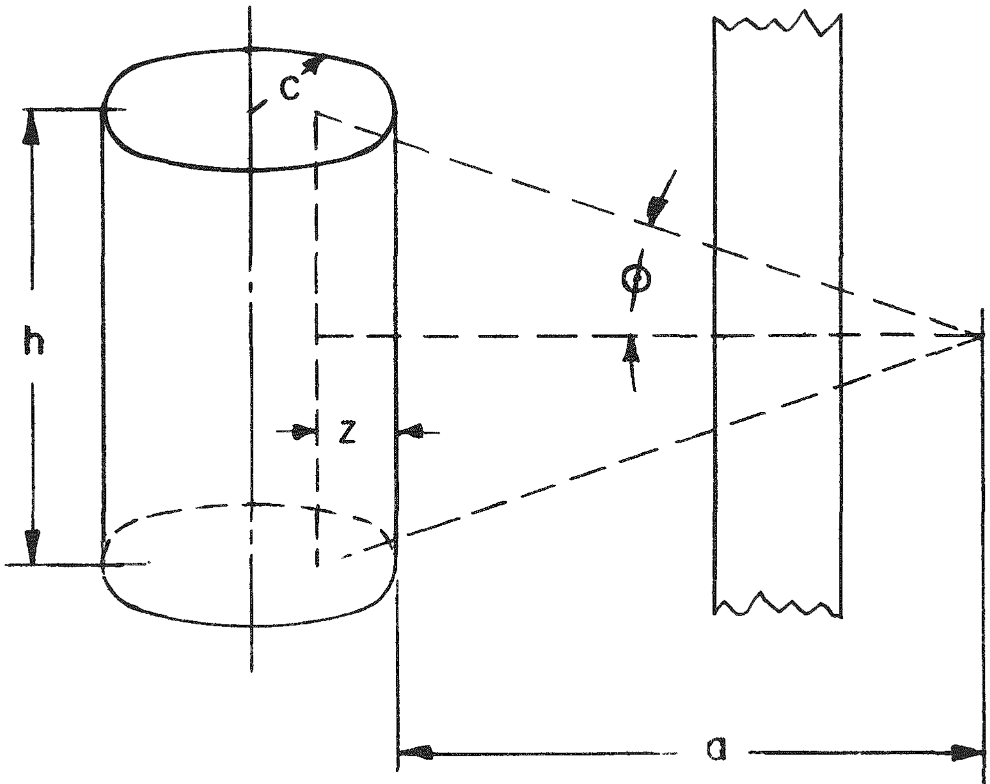

FIG. 2.1 - GEOMETRY FOR SHIELDING CALCULATION
OF CYLINDRICAL SOURCE

previously by the volume fraction of water in the steam generator.

The build-up is calculated by adding the build-up expected [10] in each material along the attenuation length, b. The build-up in concrete is determined from the build-up factor for aluminum, which has approximately the same effective atomic number as concrete. Equivalence on the basis of equal atomic number is considered the best procedure available.

The calculation of the build-up factor for the steam generator shielding is indicated below:

Shielding Component	Relaxation Lengths	Build-up Factor	Build-up
Tube Bundle	0.59	1.25	0.25
Shell Wall	1.02	1.36	0.36
Concrete	9.13	5.08	4.08
Total	10.74		4.69

Overall Build-up Factor = 5.69

The results of the calculations of dose rate from primary coolant are presented in Table 2.2. The conversion from photon flux to dose rate is determined from Reference 5.

Three feet of concrete are provided external to the vapor container to a height of 27 feet above ground level. Above this height on the upper hemispherical end of the vapor container there is no additional concrete outside the vapor container Above the vapor container only the water in the steam generator tube bundle and in the piping contribute to the dose from the primary coolant. The dose rate calculated for this location is indicated in Table 2.3. It should be noted that in addition to the dose rate of 8.5 mr/hr shown in Table 2.3, there is a dose rate of 3.1 mr/hr from the reactor (see

Table 3.4) making a total of 11.6 mr/hr above the vapor container

TABLE 2.3

DOSE RATE ABOVE VAPOR CONTAINER FROM PRIMARY COOLANT ACTIVITY DURING REACTOR OPERATION

Source	Gamma Flux photons/cm^2 - sec	Dose Rate mr/hr
Piping	740	5.7
Steam generator bundle	360	2.8
Total --------------------------------	1100	8.5

CHAPTER 3

PRIMARY SHIELD

3.1 Design

Fig. 3.1 is a cutaway drawing of the reactor and primary shield, with elevation and plan views in Figs. 3.2 and 3.3.

Outside the pressure vessel are four inches of insulation held in place by a 3/8-inch shell of steel. After a small air gap there is the inner wall of the shielding which is a two-inch steel cylinder. This inner wall of the shield tank also supports the pressure vessel below the inlet and outlet pipes. Seven steel cylinders two inches thick are arranged concentrically around the inner wall of the tank, with one inch of water between adjacent cylinders. These seven layers of steel, plus the two-inch inner wall of the tank, give a total of sixteen inches of steel radially around the reactor outside of the pressure vessel and constitute the primary gamma shield.

Above the pressure vessel, the inner wall of the shield tank forms a well, 12.5 feet deep, which is filled with water.

The inlet and outlet lines are surrounded by 4-inch annuli containing insulation, which offers low resistance to gamma penetration. Although neither pipe is in direct line with the core, a considerable amount of scattered radiation and a significant quantity of direct radiation can escape through the annuli. To prevent this streaming, blocks of steel as shown on Fig. 3.2 are added. These rings effectively stop open paths in all directions.

Tables 3.1 and 3.2 indicate the shielding materials available from the core to the outside of the primary shield in the radial and vertical directions,

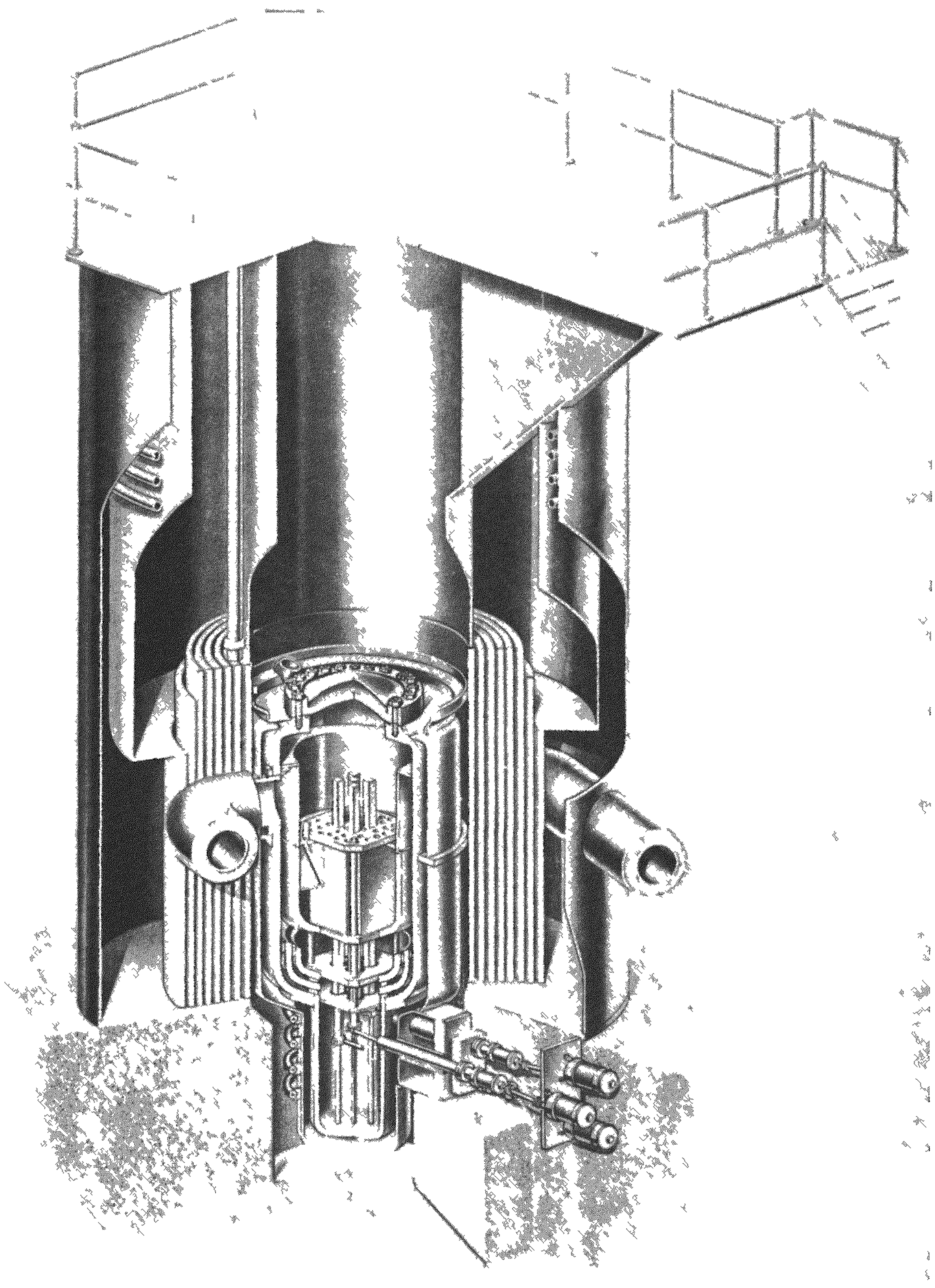

FIG. 3.1 - REACTOR AND PRIMARY SHIELD

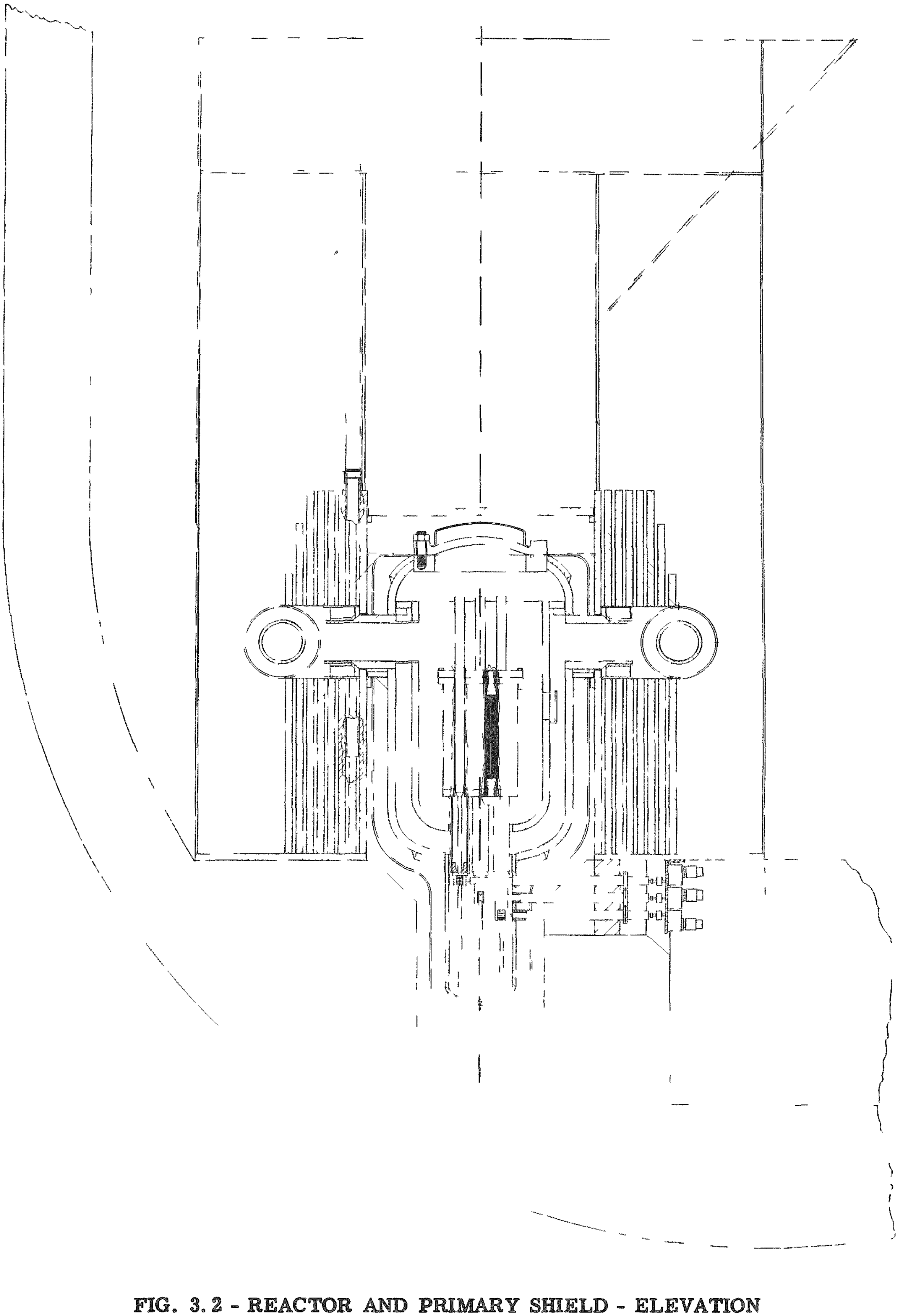

FIG. 3.2 - REACTOR AND PRIMARY SHIELD - ELEVATION

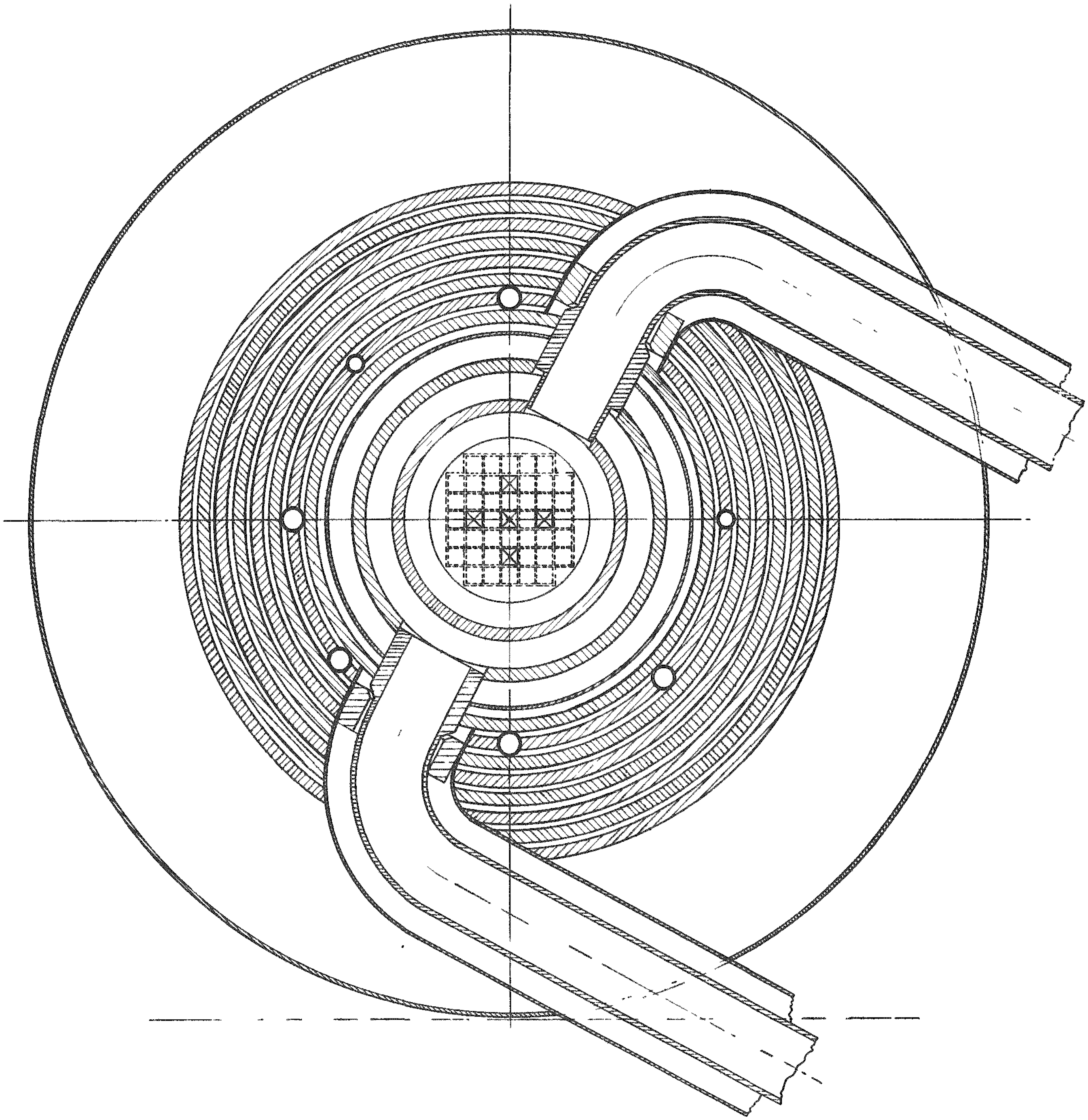

FIG. 3.3 - REACTOR AND PRIMARY SHIELD - PLAN VIEW

TABLE 3.1

DESCRIPTION OF REACTOR SHIELD - RADIAL

Description	Material	Outer Radius Inches	Thickness Inches
Core	-	11.1	-
Reflector	Primary Water	17.5	6.4
Thermal Shield	Stainless Steel (1)	19.5	2.0
Inlet Passage	Primary Water	24.0	4.5
Pressure Vessel	Steel	26.2	2.2
Insulation	Glass Wool (2)	30.2	4.0
Insulation Cladding	Steel	30.6	0.4
Clearance Space	Void	32.0	1.4
Vessel Support and Shield Tank Wall	Steel	34.0	2.0 (3)
1st Cooling Passage	Shield Water	35.0	1.0
1st Shield Ring	Steel	37.0	2.0 (3)
2nd Cooling Passage	Shield Water	38.0	1.0
2nd Shield Ring	Steel	40.0	2.0 (3)
3rd Cooling Passage	Shield Water	41.0	1.0
3rd Shield Ring	Steel	43.0	2.0 (3)
4th Cooling Passage	Shield Water	44.0	1.0
4th Shield Ring	Steel	46.0	2.0 (3)
5th Cooling Passage	Shield Water	47.0	1.0
5th Shield Ring	Steel	49.0	2.0 (3)
6th Cooling Passage	Shield Water	50.0	1.0
6th Shield Ring	Steel	52.0	2.0 (3)
7th Cooling Passage	Shield Water	53.0	1.0
7th Shield Ring	Steel	55.0	2.0 (3)
Neutron Shield	Shield Water	80.0	25.0
Shield Tank Outer Wall	Steel	80.4	0.4

(1) Considered as steel for shielding purposes.

(2) Considered as void for shielding purposes.

(3) Computed at 14.3" for the 8 - 2" layers.

TABLE 3.2

DESCRIPTION OF REACTOR SHIELD - VERTICAL

Description	Material	Distance From Center of Core Inches	Thickness Inches
Core	-	11.1	-
Reflector	Primary Water	12.6	1.5
Support Plate	Stainless Steel, Water(1)	14.6	2.0
Header	Primary Water	51.0	36.4
Pressure Vessel Cover	Steel	53.7	2.7
Insulation	Glass Wool(2)	59.6	5.9
Insulation Cladding	Steel(3)	60.0	0.4
Neutron and Gamma Shield	Shield Water	210.0	150.0

(1) Since the support plate has holes for coolant water passage, the plate is considered as water for shielding purposes.

(2) Considered as void for shielding purposes.

(3) Neglected for shielding purposes, as the material is only over a small portion of the reactor vessel.

TABLE 3.3

DOSE RATE FROM REACTOR DURING FULL POWER OPERATION-RADIAL

Location	Gamma Dose Rate mr/hr	Fast Neutron Dose Rate mrep/hr
Reactor Surface	2.2×10^{12}	1.8×10^{11}
Outside Shield Tank	6.2×10^{4}	2.6×10^{1}
Inside Vapor Container	9.8×10^{3}	4.1
Outside Vapor Container	0.75	4.6×10^{-6}
One-tenth Tolerance	0.75	7.5×10^{-2}

respectively. The primary shield is designed such that the dose rate outside the primary shield due to the reactor is approximately the same as from the primary coolant.

In the event of loss of primary shield water, it is estimated that the dose in the control room might rise to 1.2 times tolerance. This would still permit continuous reactor operation on an emergency basis if necessary.

The dose rate, with the reactor operating at 10 megawatts, from neutrons and gammas at various points in the radial and top shield are given in Tables 3.3 and 3.4. The dose from thermal neutrons outside the concrete shield is much less than the fast neutron dose. The control room, the point for which data is given, is the nearest normally occupied location to the reactor.

The shield was calculated by comparison with ORNL Lid Tank and Bulk Shielding Reactor experimental data. The BSR spectrum was corrected for the harder gamma radiation anticipated from the APPR-1 core. The attenuation through water was obtained directly from BSR data. The effectiveness of the iron in reducing gammas and fast neutrons was determined from Lid Tank data for an iron-water shield. The iron in the experimental set-up was closer to the source plate than the thermal shield is to the APPR-1 core, which assures that the secondary gammas are treated on a conservative basis. The attenuation through the secondary shield is calculated by simple exponential attenuation of the flux at the inside of the concrete. A relaxation length characteristic of 7-Mev gammas is used for the gamma flux, as it is indicated that the predominant gammas penetrating to the outside of the shield are hard.

TABLE 3.4

DOSE RATE FROM REACTOR
DURING FULL POWER OPERATION-VERTICAL

Location	Gamma Dose Rate mr/hr
Reactor Surface	2.2×10^{12}
Above Water	1.5×10^{3}
Inside Vapor Container	1.8×10^{2}
Outside Vapor Container	3.1
Tolerance	7.5

3.2 Calculation of Primary Shield for Full Power Operation

The basic method used and results obtained have been given above.

3.2.1 Comparison of Leakages from APPR-1 and BSR Cores

The leakage of fast neutrons will be less for the APPR-1 than for the BSR because of the higher removal cross-section of iron compared to aluminum. W. R. Pearce (11) calculates the relative leakage to be 0.67. This ratio is conservatively assumed as unity for these calculations.

A comparison has been made of the gamma spectrum from the BSR and APPR-1 cores. Since gammas arising from the capture of thermal neutrons are the most important in the shielding problem, a comparison has been made of the relative capture gamma spectra. Both reactors are normalized to photons produced per fission of uranium-235.

From the known compositions (11) of the cores, the absorptions per fission in each material can be determined. Cross-sections are obtained from References 12 and 13.

Reactor	Material	Core Density gm/cm^3	Absorption cross-section barns/molecule	Absorptions per fission
BSR	U-235	0.0358	580. *	-
	Al	1.12	0.215	0.101
	H_2O	0.585	0.66	0.243
APPR-1	U-235	0.083	580. *	-
	Fe	1.55	2.43	0.329
	H_2O	0.732	0.66	0.131

* Fission Cross-section

The gammas are divided into 3 energy groups, of 7, 4, and 2 Mev. The number of photons per absorption is determined (14) as:

Material	Photons per absorption in group 7 Mev	4 Mev	2 Mev
Aluminum	0.56	0.77	0.15
Water	0.00	0.00	1.00
Iron	0.72	0.24	0.10

Thus the photons produced per fission in each reactor and the ratio between the two reactors can be determined.

Reactor	Photons per fission in group 7 Mev	4 Mev	2 Mev
BSR	0.057	0.078	0.501
APPR-1	0.237	0.079	0.295
Relative production APPR-1/BSR	4.16	1.01	0.59

Using the densities as given above and gamma mass absorption coefficients given in Reference 4, coefficients can be determined for the two cores.

Reactor	Gamma Mass absorption coefficient, cm^{-1} 7 Mev	4 Mev	2 Mev
BSR	0.0421	0.0562	0.0785
APPR	0.0660	0.0797	0.1018

Self-shielding factors (15) for spheres of uniform volume source strength can be determined. The assumption of uniform strength is conservative, as the maximum source is at the center. The flux peak near the surface is only in the outer few centimeters, which is much less than the relaxation length for the gammas. The relative escape from the reactors is the ratio of the self-shielding factors. The relative source strength at each energy is the product of the relative production and the relative escape at that energy.

		Gamma Group		
	Reactor	7 Mev	4 Mev	2 Mev
Self-shielding factor	BSR	0.483	0.404	0.313
	APPR-1	0.355	0.307	0.248
Relative escape	APPR-1/BSR	0.735	0.760	0.792
Relative source	APPR-1/BSR	3.06	0.77	0.47

Since calculations indicate that the 7-Mev group is predominant outside the shield, the entire dose as measured in BSR curves is increased by the factor of 3.06.

3.2.2 Calculation of Radial Gamma Attenuation

The shield materials in the radial direction are given in Tables 2.1 and 3.1.

In comparing the BSR and APPR-1 reactors, it should be noted that the radius of a sphere having the same volume as the core is 27.6 cm for the BSR and 28 2 cm for the APPR-1. The dose rate at a given distance from the surface of a reactor of given total power is less for a larger core, since more shielding is present between the receptor and remote points of the core Thus the comparison is conservative.

The dose rate from the BSR is determined (17) at 152 cm, which is the distance through shielding material from the core to the outside of the shield, with a correction for densities of the APPR-1 primary water and shield tank water. This dose rate is 6.8×10^{-3} r/hr-watt. Since the actual distance from the APPR-1 core is greater than 152 cm, the figure given should be conservative Corrected for different relative source strength and power level, the dose rate with no shield metal present would be 2.11×10^{5} r/hr.

Iron-lead mock-ups of the STR have been tested in the ORNL Lid Tank Facility (20). The effect of replacement of water by iron and lead at 150 cm from the source plate is shown in Fig. 3.4. Considering the lead as equivalent to iron for 7 Mev Gammas gives a reasonably good curve for extrapolating the effectiveness of iron. The attenuation from 19.5" of iron slabs is 2.9×10^{-4}, giving a dose rate outside the primary shield of 6.2×10^{4} mr/hr. It should be noted that the first slab in the mock-up is 20 cm from the source, while the first steel is 13 5 cm (effective) from the APPR-1 core. However, for the rest of the slabs, the iron in the STR mock-up is closer to the core than the iron in the shield. A comparison of the location of water and steel in the two configurations is shown in Fig 3.5. Calculations by Taylor (8) and in Sec-

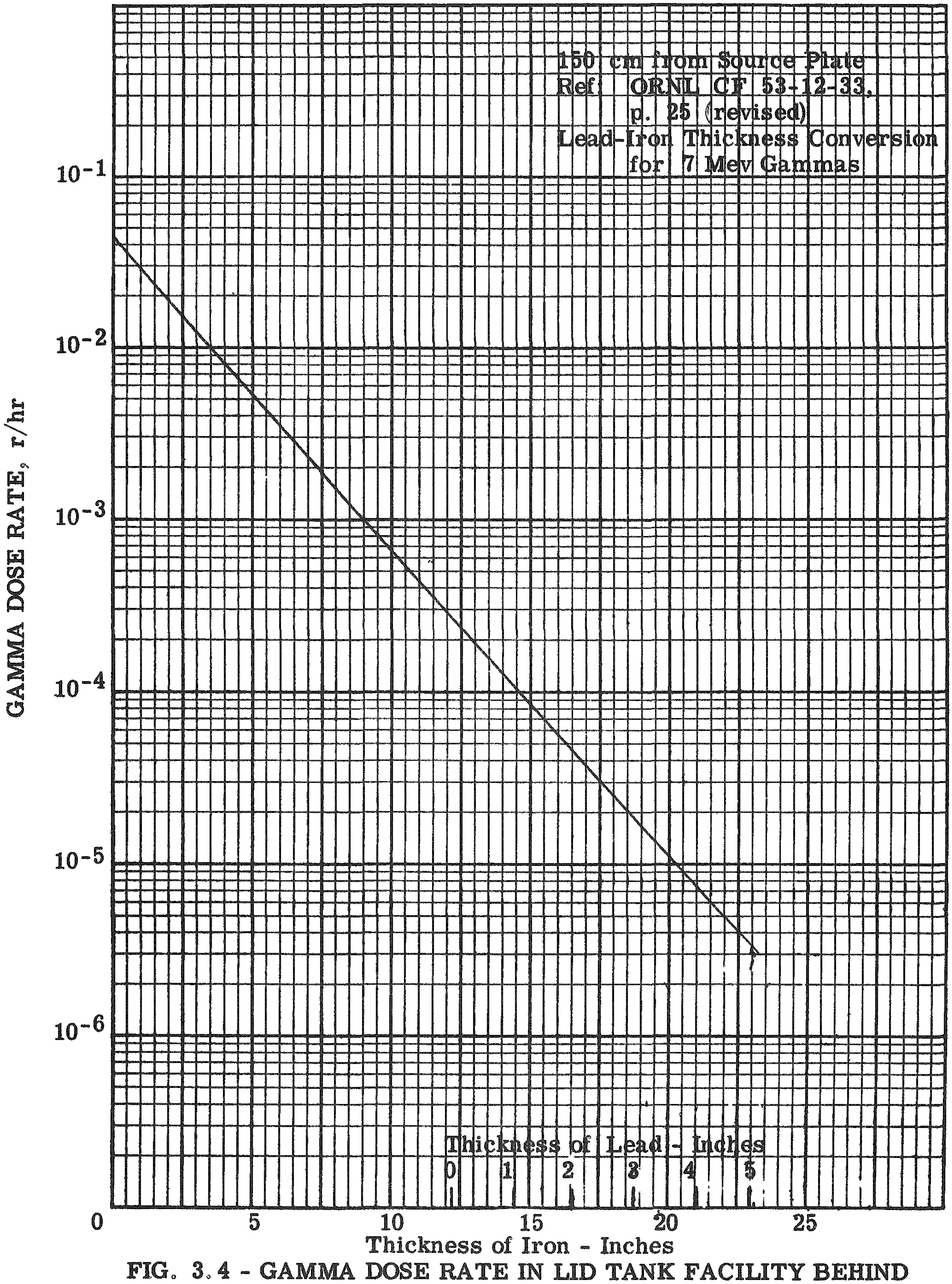

FIG. 3.4 - GAMMA DOSE RATE IN LID TANK FACILITY BEHIND IRON AND LEAD SLABS IN WATER

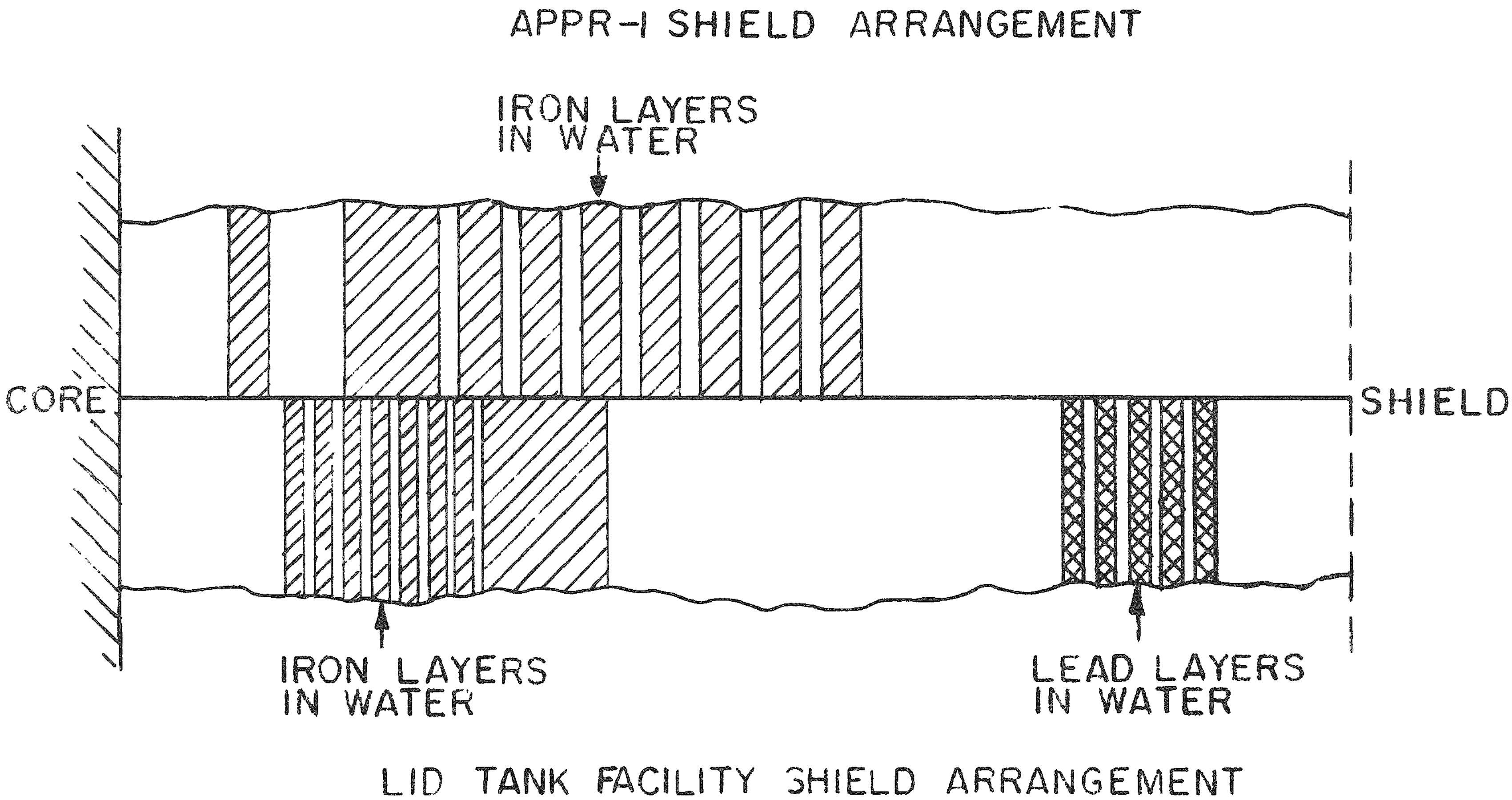

FIG. 3.5 - EFFECTIVE SHIELD CONFIGURATIONS OF APPR-1 AND LID TANK FACILITY EXPERIMENT

tion 3.3.3 indicate that the most important source of secondary gammas received outside the shield comes from the outer layers of the steel. It is believed that secondary gammas have been adequately treated in this calculation.

The dose inside the vapor container is calculated by simple inverse-square-distance from the outside of the primary shield. This is conservative for cylindrical geometry (21), as outside points not on the same elevation as the core have greater shielding from the core than points radially outward from the core. The dose rate just inside the vapor container near the control room is thus 9.8×10^3 mr/hr.

By attenuating the gamma spectrum at 147 cm in water from the BSR through 19.5" of iron and 60" of concrete, it is found that 7 Mev gammas predominate outside the shield. Thus it appears reasonable to attenuate the total dose rate inside the vapor container using a relaxation length characteristic of 7 Mev gammas. Since the spectrum already includes more low energy gammas than would be present solely from scattering of 7 Mev gammas, no build-up factor should be applied to the exponential attenuation. Slab geometry is assumed.

The absorption coefficient for concrete is obtained by extrapolation of data from reference 23, corrected for density. The coefficients used are:

Material	Gamma Mass Absorption Coefficient cm^{-1}
Iron	0.236
Concrete	0.0593

The attenuation through the secondary shield is 7.7×10^{-5}, giving a dose rate outside the vapor container of 0.75 mr/hr from the core and secondaries generated in the shield. The dose rate at various points in the radial shield is listed in Table 3 4.

3 2.3 Calculation of Axial Gamma Attenuation

The shield materials in the vertical direction are given in Tables 2.1 and 2.2.

The top shield is calculated in the same manner as the radial shield. The dose rate from the BSR (19) is determined at 475 cm, which is the distance through shielding material from the core to the top of the shield water, with a correction for the densities of the APPR-1 primary water and shield tank water. This dose rate is 1.3×10^{-7} r/hr-watt. Corrected for relative source strength and power level, the dose rate would be 4.0 r/hr with no metal present.

Using the attenuation curve for replacement of water by iron (Fig. 3.3), the dose rate above the water is 1.5 r/hr. The iron in the vertical direction is considerably further away from the core than is the iron in the experimental setup.

By the use of inverse-square-distance attenuation from the outside of the shield water to the inside of the top of the vapor container, as justified previously, the dose rate inside the vapor container is calculated to be 180 mr/hr. Using exponential attenuation through the vapor container (24 inches of concrete and 0 75 inches of iron), the dose rate directly above the vapor container is 3.1 mr/hr. The dose rate at various points is summarized in Table 3.4.

3.2.4 Calculation of Radial Neutron Attenuation

The neutron attenuation has been calculated using a method similar to that used for the gamma attenuation. The leakage per unit power, as mentioned in Section 3.2.1, is conservatively assumed equal for the APPR-1 and BSR.

The fast neutron dose from the BSR has been measured (18). The attenuation resulting from the substitution of iron for water has been obtained from Reference 20.

The geometrical correction factor for distance in air is the same as for gammas. The fast neutrons are attenuated through concrete using a measured relaxation length of 11.1 cm for a 2.3-gm/cc Portland concrete (24).

On this basis, the fast neutron dose rate outside the vapor container is 4.6×10^{-6} mrep/hr. This is 6.1×10^{-5} times tolerance. The thermal neutron dose is less than this. The dose rate at various points in the radial shielding is indicated in Table 3.3.

From Reference 23, the ratio of thermal neutron flux to fast neutron dose is approximately 220 nv_{th} per mrep/hr. Also, at large distances in water, where the photo-neutrons produced from the deuterium in natural water predominate, the ratio of gamma dose rate to thermal neutron flux is 4.7 r/hr per nv_{th}. Thus one expects the fast neutron dose rate in water (measured in mrep/hr) cannot be less than 10^{-6} times the gamma dose rate (in mr/hr). In the radial direction, the above ratio is 6×10^{-6}; hence photo-neutrons are probably not significant.

3.2.5 Calculation of Axial Neutron Attenuation

Because of the large distance of water above the reactor, the neutrons at the top of the shield are photo-neutrons produced in the water. The dose contribution is negligible compared to the gamma dose.

3.3 Comparison of Methods of Calculating Reactor Shielding During Full Power Operation

3.3.1 Equivalence of Concrete and Water for Gamma Attenuation

As a check of attenuating the gammas through concrete using a 7 Mev gamma as characteristic, the calculation performed in Section 3.2.2 was repeated with the replacement of 60 inches of concrete by 336 cm of water. This is equivalent on a density basis. The gamma mass absorption coefficients per unit density for concrete and water are nearly identical in the range of energies of interest, namely from 1 to 7 Mev.

Using BSR data (19) the attenuation through the additional 336 cm of water is 1.46×10^{-5}. The attenuation through the vapor container steel is 0.64, and with an inverse-square-distance correction factor of 0.285, the dose rate outside the vapor container is calculated to be 0.26 mr/hr. This compares to the value calculated in Section 3.2.2 of 0.75 mr/hr, indicating that the use of 7 Mev gammas as characteristic is probably conservative.

3.3.2 Core Gamma Attenuation

In an effort to check the experimental calculation of dose rate based on comparison with BSR and Lid Tank data, an analytical method has been chosen to evaluate the dose rate expected from the core.

Gammas from the core arise from four principal sources: direct fission reaction, fission products, radiative capture, and inelastic scattering. Since the hard capture gammas from structural material in the core are the major contributors to the external dose, their energies should be used in establishing energy groups into which all gammas are assigned The groups were chosen as follows:

Characteristic Gamma Energy for Group	Range of Energies Included in Group
Mev	Mev.
8	6 up
4	3 to 6
2	0 to 3

The direct fission gammas are assumed to have the distribution (25).

$$N\ (\gamma) = 7.7\ e^{-1.03E}\ \text{photons/Mev-fission}$$

These gammas are assigned to the energy groups, applying conservation of energy within each group. The number of gammas for each group is shown in Table 3.5.

The equilibrium fission product gamma spectrum (22) is given as:

$$N\ (\gamma) = 7.4\ e^{-1.16E}\ \text{photons/Mev-fission}$$

These photons are assigned to energy groups, as indicated in Table 3.5.

TABLE 3.5

ENERGY GROUP DISTRIBUTION
OF PROMPT AND FISSION PRODUCT GAMMAS

Energy Group Mev	Prompt Fission Gammas per Fission	Fission Product Gammas per Fission
8	0.014	0.005
4	0.312	0.018
2	2.953	2.367

The core capture gammas are computed for the core composition reported in Reference 21 Since the reactor is about 70% thermal, the absorptions per fission are calculated using thermal absorption cross-sections. The results are indicated below:

Material	Mass in Core Kg	Absorption/Fission
Ni	37.5	0.109
Cr	16.6	0.036
Fe	154.	0.247
U	10.8	0.184
B_4C	0.22	0.460
H_2O	92.2	0.126

The yield in each energy group (4, 26) is indicated in the table below. No data is reported from nickel, chromium or iron below 3 Mev, so the lower yields have been neglected. The low energy gammas are readily attenuated in the shield. Boron gives negligible gamma production.

Material	Photons Per Absorption 8 Mev	4 Mev	2 Mev
Ni	0.38	0.28	-
Cr	0.51	0.16	-
Fe	0.42	0.24	-
U-235	-	-	2.5
B_4C	-	-	-
H	-	-	2.2

The inelastic scattering source is expected to be small. No suitable data is available at this time, so the source from neutron captures was increased by 20%, in accordance with results of calculations in reference 8.

The total gamma source is then calculated as:

Energy Group	Photons/Fission
8	0.217
4	0.445
2	6.21

The direct and fission product gamma sources should have the same spatial distribution in the reactor core as the power distribution. The capture gammas would have the same distribution as the thermal flux, neglecting fast captures. The gamma source from inelastic scattering can probably be best approximated from the fast flux distribution. However, in view of the similarity of the thermal flux and power distributions in the APPR and the relatively small importance of the inelastic scattering, the gamma source is assumed to have the same spatial distribution as the power, obtained from Reference 7. The source thus has the same spectrum at all points in the core.

The core is divided into three coaxial cylinders with a uniform volume distributed source in each, the volume source of intensity being obtained by averaging the power distribution. Coaxial cylinders rather than concentric shells are chosen as they can be used directly with an effective self-absorption distance (9).

The cylinders are considered as point sources with the source point located at the effective self-absorption distance. Exponential attenuation is used through the shield materials, using the following gamma mass absorption coefficients:

Material	Mass Absorption Coefficient, cm^{-1} for Energy Group		
	8 Mev	4 Mev	2 Mev
Core	0 063	0.074	0.096
Primary Water	0.019	0.027	0.040
Iron	0.236	0.259	0.314
Shield Water	0.022	0.032	0.046
Concrete	0.0556	0.0737	0.113

The build-up is calculated in the same manner as described in Section 2.3. The conversion from photon flux to dose rate is based on Reference 5.

The results of the calculation are presented in the table below:

Energy Group Mev	Dose Rate Outside Vapor Container, mr/hr	
	Radial	Axial
8	0.15	44
4	Negligible	1
2	Negligible	Negligible
Total	0.15	45

3 3.3 Importance of Capture Gammas in Iron Shield

In an effort to evaluate the relative importance of capture gammas in the radial iron shield to the gammas coming directly from the core, calculations made on a similar shield configuration are useful.

The composition and location of the core, thermal shield, and pressure vessel are the same as in the design listed in Table 3 1, except that one inch was added to the pressure vessel thickness. The shield was 47 inches thick, with the inner 23.5 inches considered as homogeneous iron and water, with

72 volume per cent iron. The outer half of the shield tank was pure water. This shield design corresponds approximately to a shield with 9 two-inch steel layers separated by 0.81 inch of water, in contrast to the present shield of 8 steel slabs separated by one inch of water.

The neutron spatial distribution is determined for a single fast group. This is obtained for water by using Bulk Shielding Facility data, corrected for geometry by the appropriate transformations.

For the iron slabs in water, a two-group neutron calculation was made of a 2" iron slab preceded and followed by infinite water layers The fast neutron distribution was based on a relaxation length of 10.7 cm in water and a measured removal cross-section of 1.9 barns for iron. The thermal flux in the water deviates from an exponential only within a few inches of the iron slab. It was found for the 2" layer with the above conditions, there are 2.62 thermal captures for every removal in the iron from the fast group.

In view of the small diffusion length and "age" of neutrons in water and iron-water mixtures, it is assumed in the homogeneous shield region that the neutrons slow down and are captured at the point of removal from the fast group. To account for inelastic scattering gamma sources, 20% is added to the capture gamma source, following the same basis used in Section 3.3.2.

With the location of the captures known from the neutron distribution and the gamma spectrum as used in Section 3.3.2, the shield can be divided into regions which are sufficiently small that they can be regarded as point sources for the gamma radiation.

The 47" shield region was divided into 8 regions radially and 24 segments circumferentially A study has been made which indicates an error of no more than 5% should result from the angular location of these segments. The point source for each region is taken at a radius equal to the average of the inner and outer radii of the region. The distance from this point through outer shield materials is determined graphically.

Using the distances in each region, the exponential attenuation is computed for each source point For a shield design with water on the outside, it appears that the best convenient technique in selecting a buildup factor is to base it on the average atomic number of the shield material. This number is approximately eight

The table below indicates the ratio of gammas in each energy group from secondary (extra-core) sources to those from the core, at a point outside the shield. The dose from the 4-Mev group is less than 2% of the dose from the 8-Mev group, for the core gammas.

RATIO OF SECONDARY TO CORE GAMMAS RECEIVED OUTSIDE SHIELD

Secondary Source	Energy Group, Mev 8	4
Thermal Shield	14%	4%
Pressure Vessel	6%	3%
Homogeneous Water and Iron Region	49%	36%
Total Secondaries	69%	43%

3.3 4 Comparison of Results of Methods Used

The table below summarizes the results of the various methods of calculation of dose rate outside the vapor container for the radiation, originating in the core. The radiation from the water in the system external to the primary shield is not included.

Method	Gamma Dose Rate mr/hr Radial	Axial
Section 3.2.2, 3.2.3: Comparison with BSR, with correction for core gamma production; iron attenuation based on Lid Tank Facility data; exponential attenuation through concrete.	0.75	75
Section 3.3.1: Same as above, except concrete attenuation based on BSR data for water of equal mass thickness.	0.26	--
Section 3.3.2: Core gammas only, calculated using three gamma energy groups; Capture, fission and fission product gamma spectra from reported data; exponential attenuation through shield, corrected for build-up.	0.15	45

CHAPTER 4

SHIELDING AFTER SHUTDOWN

4.1 Shielding of Reactor Core after Shutdown

The gamma dose rate inside the vapor container and outside the primary shield determines the accessibility of the equipment for inspection and repair. This dose is calculated by dividing the fission product activity into 3 energy groups: 0.10-0.90 Mev, 1.10-1.65 Mev, and 1.80-2.90 Mev. The strength of each group for various periods of reactor operation and time after shutdown is determined from Reference 27.

The following gamma absorption coefficients are used (4).

Gamma Energy Mev	Gamma Absorption Coefficient, cm^{-1}		
	Water	Iron	Core
0.5	0.097	0.645	0.195
1.5	0.058	0.369	0.113
2.5	0.044	0.291	0.088

The dose rate from each group is computed using the shield configuration given in Table 3.1. The core is considered as a point source located at an effective self-absorption distance (9) from the actual core surface. Linear buildup factors used are conservative for the 2.5 Mev group, which is by far the most significant contributor to the dose rate outside the primary shield.

The results of the calculation are presented in Table 4.1.

TABLE 4.1

DOSE RATE OUTSIDE RADIAL
PRIMARY SHIELD FROM FISSION PRODUCT ACTIVITY

	Time After Shutdown Hours	Time of Operation: Infinite	1000 Hours	100 Hours
		Dose Rate, MR/HR		
Regular Shield	5	1.4	0.9	0.4
	12	1.2	0.7	0.3
	24	1.0	0.6	0.2
No Water in Shield	5	111	76	33
	12	98	63	24
	24	84	54	15

4.2 Radiation from Primary Coolant After Shutdown

4.2.1 Specific Activity of Water at Shutdown

The impurities in the primary coolant water are calculated to be:

Element	PPM	Element	PPM
C	0.082	Cl	0.137
N	0.004	Ca	0.256
F	0.002	Fe	0.232
Na	0.131	Cr	0.223
Mg	0.019	Mn	0.024
Si	0.495	Ni	0.105
S	0.290	Total	2.000

The above values are based on 1 PPM introduction with the make up water and 1 PPM addition via corrosion and/or erosion. The impurities are assumed to occur in the same proportion as they are present in the supply water (28) or as they result from corrosion (29).

All nuclides of these impurities were investigated to determine whether, when subjected to the neutron and gamma fluxes in the reactor, they would contribute to the gross activity of the coolant. The only reactions neglected were those where absorption cross-sections were unknown or where half-lives were not listed.

The equation (3) used to calculate the activity produced in the reactor is:

$$A_o = N_c \; R \, \phi \, \sigma_a \, (1 - e^{-\lambda \; T_B})$$

for activation of impurities and the equation (30) used to calculate the activity produced by recoil is:

$$A_o = \frac{A L \sigma_a \; N_m \phi}{4 \, V_c} \quad \left(\frac{\lambda}{\lambda + \frac{1}{T_B}} \right)$$

Where:

A_o = induced activity, d/s/cc.

N_c = concentration of nuclides in coolant, nuclides/cm^3

N_m = concentration of nuclides in fuel element cladding, nuclides/cm^3

R = fraction of time nuclides in the coolant would be in reactor flux

ϕ = thermal neutron flux, n/cm^2-sec.

σ_a = absorption cross-section of nuclide, cm^2

λ = decay constant of activated nuclide, hr^{-1}

A = heat transfer area in core, cm^2

L = average range of atom recoil, cm

V_c = volume of primary system cm^3

T_B = average time nuclide is in primary system, hr.

The activity from recoils results from neutron captures in the outer part of the fuel plates. The recoil of the excited nucleus has a probability of entering the primary coolant of 0.25, if it starts from a point where the average range of the recoil atom in the metal is less than the distance to the liquid.

Values for A and L are obtained from Reference 11, and for σ_a and λ from Reference 31.

The active nuclides which will contribute to the gross activity after shutdown are listed below with the calculated values of A_o.

Nuclide	Specific Activity dis/cm^3-sec	Half-life
Na^{24}	2.97×10^3	14.9h
P^{32}	23.4	14.3d
S^{35}	1.5	87d
Ca^{45}	0.6	152d
Cr^{51}	3.47×10^3	26.5d
Mn^{56}	1.08×10^5	2.6h
Fe^{59}	49.9	47d
Ni^{59}	0.2	2×10^5y
Ni^{63}	7.6	85y

4.2.2 Dose Rate Expected from Water Activity

With the volume source strength computed above and for periods of time between 6 minutes and 48 hours, sodium-24 and manganese-56 are the only significant contributors to the dose. Chromium-51 has a 0.51 Mev gamma.

It is found convenient to assume the 2.8 Mev (100% yield) and the 1.4 Mev (100% yield) gammas from sodium-24 equivalent to 3 Mev gammas at 140% yield. The effective volume source strengths at shutdown can then be computed, assuming cold water in the primary system.

Nuclide	Photon Energy Mev	Specific Activity Photons/cm^3-sec
Na^{24}	3	5.0×10^3
Mn^{56}	2	5.2×10^4

Two volume sources of radiation were considered: the steam generator tube bundle, and piping. The description of these volume sources is given in Section 2.3.

The only shielding is the wall of the steam generator shell or piping. The method of calculation of the dose rate, the wall thickness, and the gamma absorption coefficients are described in Section 2.3. The dose rate is calculated for a point immediately adjacent to the piping and to the steam generator.

By coincidence, it is found that the dose rate at any given time after shutdown is the same outside either the piping or the steam generator. The results of the calculation are presented below:

Time After Shutdown Hours	Gamma Flux, Mev/cm^2-sec, from Sodium-24	Manganese-56	Total Dose Rate mr/hr
0.1	47,000	264,000	478
1	45,000	202,000	382
12	27,000	11,700	56
24	15,000	440	23
48	5,100	1	7.4

4.3 Shielding During Spent Fuel Element Transfer and Storage

Spent fuel elements must be shielded during removal from the core, transfer to the spent fuel element storage pit, and storage in the pit.

The gamma dose rate from a spent fuel element with water shielding is calculated by dividing the fission product energy into 3 energy groups: 0.10 - 0.90 Mev, 1.10 - 1.65 Mev, and 1.80 - 2.90 Mev. The strength of each group for 24 hours after shutdown from continuous reactor operation is determined from Reference 27.

The fuel element is considered as a point source, with no advantage taken for self-shielding. The fuel element calculated has operated at twice the average fuel element power, or 445 KW. The effective point source strength is listed below:

Energy Group Mev	Source Strength Mev/sec
1.5	1.8×10^{15}
2.5	2.0×10^{14}

The dose rate from the 0.5 Mev energy group is negligible.

The gamma absorption coefficients for water are listed in Section 4.1. Buildup factors are obtained from Reference 10.

Table 4.2 indicates the dose rate expected from one used fuel element 24 hours after shutdown from 1000 hours of continuous operation, with various thicknesses of water shielding. It is expected that the most active element would have an activity twice the average activity.

Lead shielding surrounds the fuel element transfer tube to protect personnel at the fuel handling position while the fuel element is in the transfer tube.

The water level in the spent fuel storage pit must be the same as in the top shield tank when the transfer tube is open. Thus, there is more than 20 feet of water above the fuel elements in the storage pit. This is completely adequate, as Table 4.2 indicates.

TABLE 4.2

DOSE RATE ABOVE WATER FOR A USED FUEL ELEMENT

The fuel element is removed 24 hours after shutdown from infinite operation. The fuel element is assumed to have twice the fission product activity of an average element. The thickness of water is measured to the nearest point of the active core section.

Thickness of Water Feet	Dose Rate mr/hr
8	270
9	57
10	12
11	2.7
12	0.62

CHAPTER 5

ALTERNATE SHIELD DESIGNS

5.1 Metal-Water Shields

An investigation of the use of lead instead of iron cylinders in the primary shield tank has been considered. Using Lid Tank data (32), (33), it is found that the shields described in Table 5.1 are equivalent in reducing the dose in the Lid Tank Facility. It is expected that the iron shield would be slightly more effective in reducing the dose from a stainless steel core, with its associated harder gammas. It might be expected that the lead which has a minimum in its gamma cross-section at 3 Mev, would produce a gamma dose of mostly 3-Mev gammas outside the concrete. However, it is found by calculation that the dose will still result from the harder photons, about 6-7 Mev. Hence no advantage can be taken of basing the concrete thickness on 3-Mev gammas rather than 7-Mev photons as the greatest dose contributor outside the concrete.

The weights of the various radial shields, assuming all metal 9 feet high, are given in Table 5.1. An inner radius of 32" is used for the innermost iron cylinder. Using a cost for material of ten cents per pound for steel and 16 cents per pound for lead, the estimated costs of the various shield configurations are also indicated in the same table. It is expected also that the total fabrication and erection cost would be greater for the lead shield than for the steel.

TABLE 5.1

EQUIVALENT METAL-WATER SHIELD CONFIGURATION

Shield Design	Estimated Weight, Thousand Pounds Iron	Lead	Total	Estimated Material Cost Thousand Dollars
A. Iron-Water Shield, using iron shield to support pressure vessel.				
1. 13.3" of iron in 7-1 9" cylinders separated by 1" of water.	108	0	108	10.8
2. 13.3" of iron in 1-13.3" cylinder.	99	0	99	9.9
B. Lead-Water Shield, with 1" iron cylinder to support pressure vessel.				
1. 1" of iron in inner cylinder; 6.3" of lead in 6-1.05" cylinders separated by 4.6" of water (18% lead - 82% water by volume); 1" of water between iron and lead.	6	85	91	14.2
2. 1" of iron in inner cylinder; 8" of lead in 8-1.00" cylinders separated by 2.7" of water (27% lead - 73% water by volume); 1" of water between iron and lead.	6	105	121	17.4

5.2 Concrete Shield

To compare the concrete and iron-water shields, an iron-water shield with 18" of iron and 30" of primary water was compared with an equivalent concrete shield, using concrete of density 2.3 gm/cm^3 (144 lbs/ft^3).

The attenuation in water and concrete was obtained from BSR data, using water as equivalent to concrete for equal mass. This method is discussed in greater detail in Section 3.3.1. The appropriate inverse-square-distance correction has been made to the iron-water shield to correct it to the dose rate at the distance corresponding to the outside of the concrete primary shield.

Likewise in the axial direction, a concrete shield was designed for equivalence to the APPR-1 design configuration.

It is found that the concrete is 63" thick radially with a 62" cover. The difference between the two shields is indicated schematically in Figure 5.1.

Table 5.2 lists the weight which would have to be transported if materials are not available at the site. If sand, gravel and water are all available, the concrete shield will require only 14.7 tons against 66.8 tons of iron. However, if sand or additional materials must be transported, the iron shield has definite advantages. The ease and speed of erection of prefabricated steel shielding is also considered in the shield selection.

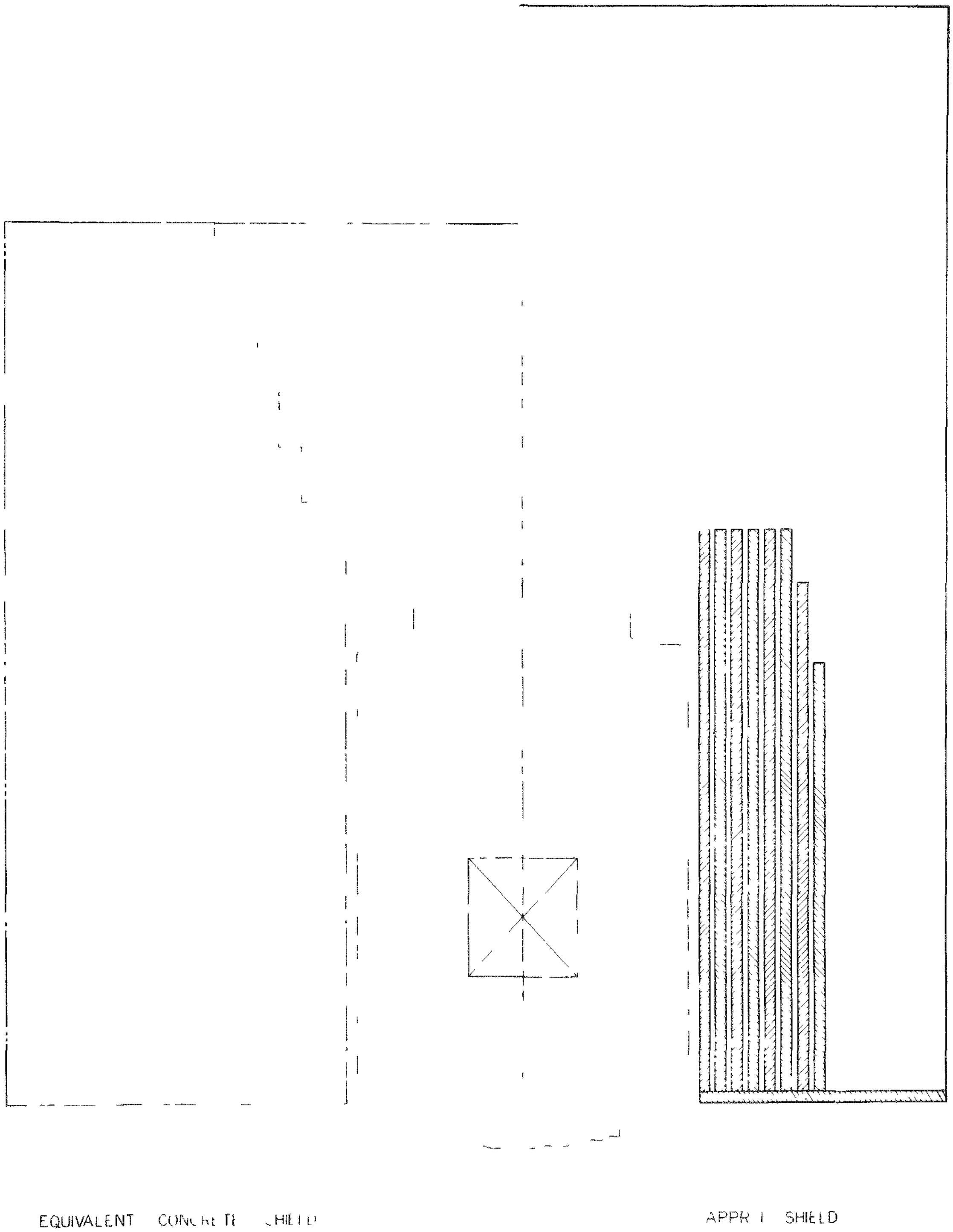

FIG. 5.1 - CONCRETE AND IRON-WATER SHIELD COMPARISON

TABLE 5.2

VARIATION OF TRANSPORTED WEIGHT OF PRIMARY SHIELD WITH MATERIALS AVAILABLE AT SITE

Shield Type	Materials Transported	Weight Tons
Iron Shield		
	Iron	66.8
	Iron, Water	74.8
Concrete Shield		
	Cement	14.7
	Cement, sand	61.2
	Cement, sand, gravel	167.4
	Cement, sand, gravel, water	179.4

CONFIDENTIAL

CHAPTER 6

GAMMA AND NEUTRON HEAT GENERATION IN SHIELD

6.1 Radial Shield

In order to calculate the leakage of energy from the core to the shield tank, it is felt that a reasonable approximation can be made by first determining the neutron and gamma fluxes outside the pressure vessel at the reactor mid-plane. The fluxes at this location are found from BSR data corrected for APPR-1 core properties and power level, and for the iron thermal shield and pressure vessel. Assuming that the fluxes determined in this manner have come from a point source at the center of the core, a correction for heat leakage into an infinite cylinder is made.

6.1.1 Gamma and Neutron Fluxes Outside Pressure Vessel

The gamma spectrum at 20 centimeters in water is obtained from a plot of F. C. Maienschein's data (36). The dose calculated from the above spectrum agrees with the measured dose from the BSR (17). A plot has been made of the APPR-1 core spectrum correction which was determined in previous shielding calculations at 2, 4 and 7 Mev. Values for other energies were obtained from this curve. A correction was made for the 4.2" total of iron in the thermal shield and pressure vessel, assuming exponential attenuation for each energy level. The gamma spectrum calculated for the surface of the APPR-1 pressure vessel is given below:

Energy Mev	Gamma Flux Photons/cm^2-sec-Mev-watt
1	1.4×10^4
2	50.9
3	28.2
4	12.9
5	9.9
6	7.8
7	9.9

The fast neutron dose at 30 cm from the BSR is obtained from Reference 19. The 30 cm represents the total water thickness corrected for density plus the total iron thickness. No additional fast neutron removal is assumed in the iron. It is estimated that there are 4.9 relaxation lengths from the surface of the reactor to the outside of the pressure vessel. The dose rate is converted to fast neutron flux using the figure of 66.7 n/cm^2-sec. per mrep/hr.

6.1.2 Leakage from a Point Source within an Infinite Cylinder

The diagram below shows the geometry used.

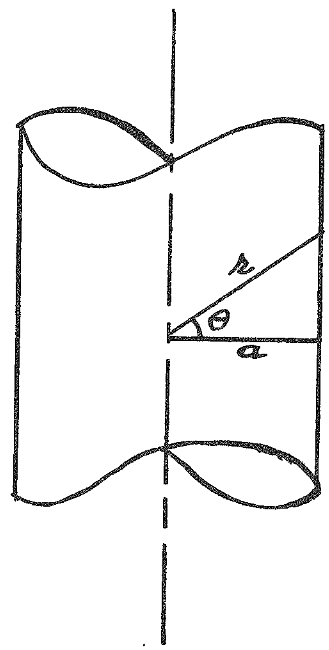

Assuming exponential attenuation from the point source, the total leakage from an infinite cylinder of radius "a" is given by:

$$N_c = 2S \int_0^{\pi/2} \frac{e^{-\mu r}}{4\pi r^2} \; 2\pi r \quad a \; d\theta$$

where:

S = point isotropic source strength

μ = absorption coefficient for radiation

The integral for N_c can only be evaluated numerically. However, for gammas it is reasonable to assume a linear build-up factor,

$$B = \mu r$$

In this case the ratio $\frac{Nc}{Ns}$ can be written in the form

$$\frac{Nc}{Ns} = \frac{\int_0^{\pi/2} e^{-\mu a \sec\theta} \, d\theta}{e^{\mu a}}$$

A curve for the integral in the numerator is given in Reference 13, where $b = \mu a$. This ratio of the leakage from a cylinder to the leakage from the inscribed sphere has been computed and plotted against μa in Fig. 6.1.

6.1.3 Energy Received in Shield Tank

The geometrical correction factor obtained from the previous section is used to correct the leakage spectrum at the outside of the pressure vessel. Using the area of a sphere with a 26.2" radius, the total energy flux is 12.7×10^9 Mev/sec - watt, or at full power, 12.7×10^{16} Mev/sec. This equals 72,000 BTU/hr.

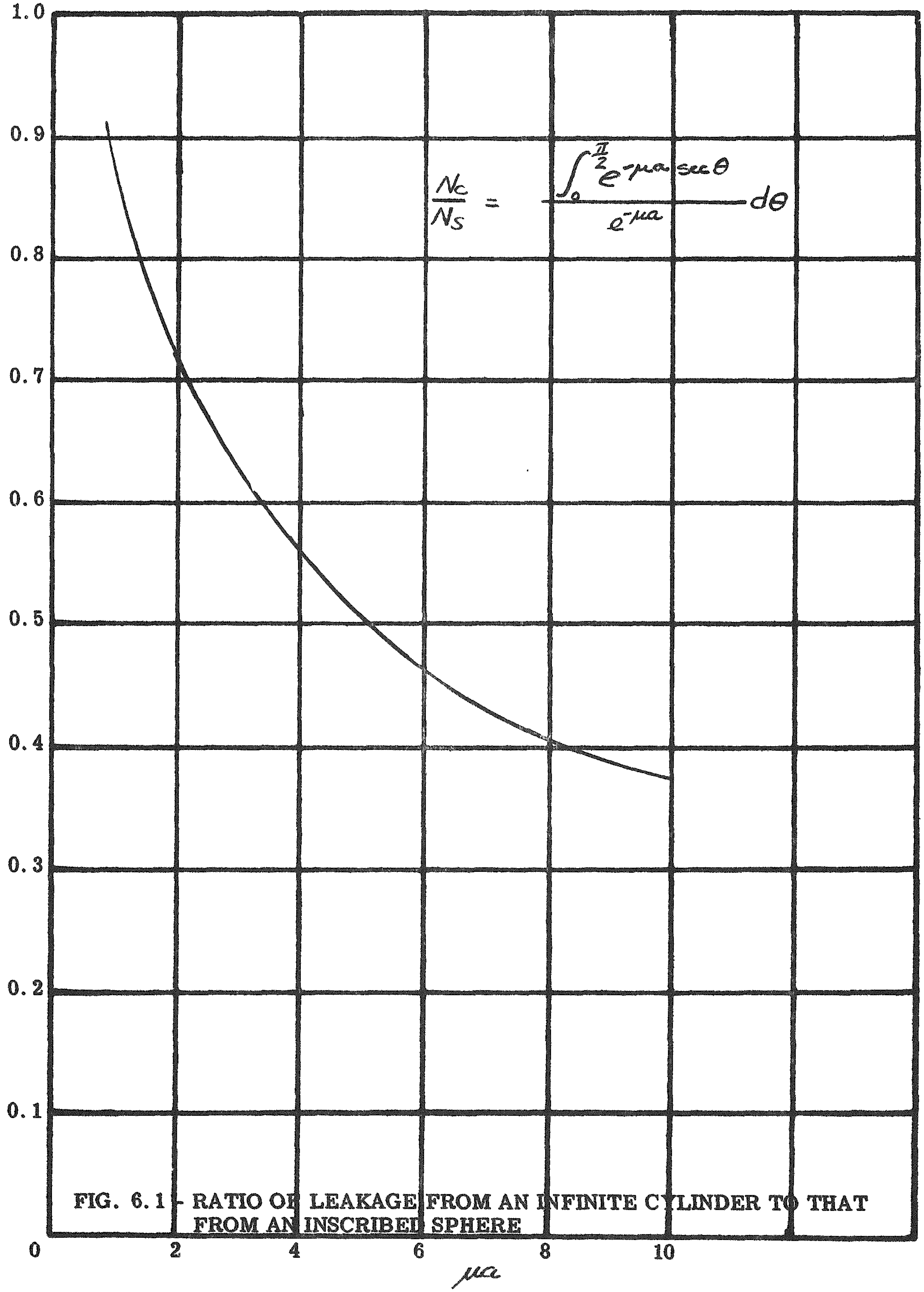

FIG. 6.1 - RATIO OF LEAKAGE FROM AN INFINITE CYLINDER TO THAT FROM AN INSCRIBED SPHERE

Although it is not accurate to do so, the same geometrical correction factor obtained above for gammas can be used for neutrons, since it is found that the total energy from the neutrons is appreciably lower than from core gammas. The total neutron leakage calculated in this way is 3.0×10^8 n/watt-sec. Assuming each fast neutron contributes 7 Mev in slowing down and in capture gammas, the total energy is 2.1×10^9 Mev/watt-sec., or at full power 2.1×10^{16} Mev/sec. This equals 12,000 BTU/hr.

The total heating in the radial shield tank is 84,000 BTU/hr.

6.2 Top and Bottom Shields

The presence of concrete used for structural purposes below the pressure vessel imposes a limit on the gamma heating which may be allowed to enter the concrete. This limit has been set at an energy flux of 50 BTU/hr-ft^2 (9.56×10^{10} Mev/sec-cm^2). In order to achieve this low value, six inches of steel is located inside the pressure vessel below the core in the space outside the control rod operating area. To stop radiation directed straight down, a 3 inch layer of steel is used, with holes for penetration of control rods.

No limitations on heating above the core exists.

Using the same procedure as for the radial shield heating, the gamma spectra has been calculated for three locations. The gamma and neutron fluxes are assumed uniform at any horizontal cross section. The errors in this assumption are probably not great, and any refined calculation of this problem appears extremely difficult. The spectra have been determined just above the pressure vessel cover, outside the pressure vessel below the inlet plenum chamber, and below the control rod drive extension of the pressure vessel. The water spectrum has been corrected for 2.9, 9.9 and 4.5 inches of iron respectively at the three locations The calculated spectra are indicated below:

	Gamma Flux, photons/cm^2-sec-Mev-watt		
Energy Mev.	Above Pressure Vessel Cover	Below Pressure Vessel Inlet Plenum Chamber	Below Control Rod Drive Extension
1	2.3×10^3	0.3×10^2	0.8×10^3
2	9.2	3.7	3 0
3	5.9	3.3	2 4
4	2.9	2.8	1.7
5	2.3	2.4	1.5
6	1.8	2.2	1 2
7	2.3	2 7	1.5

The total radiation energy entering each location with the reactor operating at full power is given below:

	Energy Flux		Total Gamma Heating
Location	Mev/sec-cm^2	BTU/hr-ft^2	BTU/hr
Above Pressure Vessel	8.8×10^{11}	462	10,300
Below Pressure Vessel Inlet Plenum Chamber	4.4×10^{10}	23	440
Below Control Rod Drive Extension	7.3×10^{10}	38	120

The neutron heating, calculated on the same basis as for radial neutron heating, is shown in the table below:

Location	Energy Flux BTU/hr-ft^2	Total Neutron Heating BTU/hr
Above Pressure Vessel	0.1	2
Below Pressure Vessel Inlet Plenum Chamber	5.4	103
Below Control Rod Drive Extension	Negligible	

REFERENCES FOR APAE-3

(1) Cochran, R. C., Neutron Spectroscopy, Reactor Shielding Information Meeting, WASH-145, p. 6 (1953).

(2) Martin, H. C., Cross Sections for the 0^{16} (n, p) N^{16} Reaction from 12 to 18 Mev, Phys. Rev., 93 (3) 498 (1954).

(3) Binford, F. T., A Method of Estimating the N^{16} Content in the Cooling System of an MTR Type Reactor, Nuclear Science & Technology, Vol. 1, No. 2, TID-2017 (1955).

(4) Blizzard, E. P., Introduction to Shield Design, CF 51-10-70 (1951).

(5) Ibid, Part 1, p. 41.

(6) Boch, A. L., et al, A Conceptual Design of a Pressurized Water Package Power Reactor, ORNL 1613 (1954).

(7) Boch, A. L., et al, A Conceptual Design of a Pressurized Water Package Power Reactor, Supplement 1, ORNL 1613, Supplement 1. (1954).

(8) Taylor, J. J., STR Shield Design, WAPD 23 (1951).

(9) Materials Testing Reactor Project Handbook, ORNL 963, Appendix 8 (1952).

(10) Goldstein, H. and J. E. Wilkins, Calculations of the Penetration of Gamma Rays, NYO 3075 (1954).

(11) Pearce, W. R., Analysis of Biological Shielding and Thermal Shielding Requirements for the ORNL Package Power Reactor, CF 53-10-81 (1953).

(12) Neutron Cross-sections, AECU 2040 (1952).

(13) Neutron Cross-sections, BNL 250 (1954).

(14) Mittelman, P., Gamma Rays Resulting from Thermal Neutron Capture, NDA 10-99 (1953).

(15) Storm, M. L., H. Hurwitz and G. M. Roe, Gamma-Ray Absorption Distributions for Plane, Spherical, and Cylindrical Geometrics, KAPL 783 (1952).

(16) Meem, J. L. and H. E. Hungerford, Unit Shield Experiments at the Bulk Shielding Facility, ORNL 1147 (1952).

(17) Ibid, p. 150.

(18) Ibid, p. 145.

(19) Flyn, J. D., Attenuation of Gamma-Ray Dose Rate and Thermal-Neutron Flux From the BSR Through Large Thicknesses of Water, WASH 292 (Pt.3), p.8 (1955).

(20) Aircraft Nuclear Propulsion Project Quarterly Progress Report, ORNL 768 (1950).

(21) Report of the 1953 Summer Shielding Session, ORNL 1575, p. 120 (1953).

(22) Ibid, p. 234.

(23) Reactor Handbook, Vol. 1, RH-1, p. 886 (1953).

(24) Ibid, p. 790.

(25) Gamble, R. L., Physics Division Semiannual Progress Report, ORNL 1620, p. 15.

(26) Kinsey, B. B. and G. A. Bartholomew, Neutron Capture Gamma-Rays from Titanium, Chromium, Iron, Nickel and Zinc, Phys. Rev., 89 (2).

(27) Moteff, J., Fission Product Decay Gamma Energy Spectrum, APEX 134.

(28) Contract between American Locomotive Co. and U. S. Atomic Energy Commission for Army Package Power Reactor, Contract AT (11-1) - 318, Appendix F (1954).

(29) Passarelli, W. O., A Study of Ventilation Requirements for Power Reactors, AECD 3228 (1951).

(30) Pearce, W. R., Analysis of Water Activation and Component Shielding for the ORNL Package Reactor Power Plant, CF 53-10-168 (1953).

(31) National Bureau of Standards, Nuclear Data, NBS Circular 499 and Supplements (1950).

(32) Index of Lid Tank Experiments 1 through 50 and some Typical Shielding Measurements, CF 53-12-33, p. 25 (Revised) (1953).

(33) Ibid, pp 19 (Revised), 21.

(34) Aircraft Nuclear Propulsion Project Quarterly Progress Report, ORNL 1294, pp 58, 65 (1952).

(35) Ibid, pp 66-68.

(36) Maienschein, F. and J. Love, Gamma-Ray Spectrum of the Bulk Shielding Reactor, Nucleonics, 12 (5) 6 (May 1954).